Exp Brain Res (2011) 212:1–18
DOI 10.1007/s00221-011-2692-1

RESEARCH ARTICLE

Age-related changes in optimality and motor variability: an example of multifinger redundant tasks

Jaebum Park · Yao Sun · Vladimir M. Zatsiorsky · Mark L. Latash

Received: 8 February 2011 / Accepted: 6 April 2011 / Published online: 26 April 2011

Abstract We used two methods, analytical inverse optimization (ANIO) and uncontrolled manifold (UCM) analysis of synergies, to explore age-related changes in finger coordination during accurate force and moment of force production tasks. The two methods address two aspects of the control of redundant systems: Finding an optimal solution (an optimal sharing pattern) and using variable solutions across trials (covarying finger forces) that are equally able to solve the task. Young and elderly subjects produced accurate combinations of total force and moment by pressing with the four fingers of the dominant hand on individual force sensors. In session-1, single trials covered a broad range of force–moment combinations. Principal component (PC) analysis showed that the first two PCs explained about 90% and 75% of finger force variance for the young and elderly groups, respectively. The magnitudes of the loading coefficients in the PCs suggested that the young subjects used mechanical advantage to produce moment while elderly subjects did not (confirmed by analysis of moments produced by individual digits). A co-contraction index was computed reflecting the magnitude of moment produced by fingers acting against the required direction of the total moment. This index was significantly higher in the young group. The ANIO approach yielded a quadratic cost function with linear terms. In the elderly group, the contribution of the forces produced by the middle and ring fingers to the cost function value was much smaller than in the young group. The angle between the plane of experimental observations and the plane of optimal solutions (D-angle), was very small (about 1.5°) in the young group and significantly larger (about 5°) in the elderly group. In session-2, four force–moment combinations were used with multiple trials at each. Covariation among finger forces (multifinger synergies) stabilizing total force, total moment, and both was seen in both groups with larger synergy indices in the young group. Multiple regression analysis has shown that, at higher force magnitudes, the synergy indices defined with the UCM method were significantly related to the percent of variance accounted by the first two PCs and to the D-angle computed using the ANIO method. We interpret the results as pointing at a transition with age from synergic control to element-based control (back-to-elements hypothesis). Optimization and analysis of synergies are complementary approaches that focus on two aspects of multidigit coordination, sharing and covariation, respectively.

Keywords Aging · Redundancy · Inverse optimization · Synergy · Finger · Force

Introduction

Many physiological changes occur within the neuromotor system with advanced age (Grabiner and Enoka 1995; Levinson 1978; Welford 1984). These include reduction of muscle mass (Doherty and Brown 1997; Rogers and Evans 1993), slowing down of muscle contractions (Cole 1991; Francis and Spirduso 2000; Seidler–Dobrin et al. 1998), impairment of tactile sensitivity (Cole et al. 1999; Verrillo 1979), and neuronal loss in a number of structures within the central nervous system (CNS) leading to plastic changes within the CNS (Booth et al. 1994; Brooks and Faulkner 1994; Eisen et al. 1996; Erim et al. 1999; Dinse

J. Park · Y. Sun · V. M. Zatsiorsky · M. L. Latash (✉)
Department of Kinesiology, The Pennsylvania State University, Rec.Hall-268N, University Park, PA 16802, USA
e-mail: mll11@psu.edu

2006). All these changes can potentially contribute to impaired motor coordination in elderly persons.

Advanced age leads to deterioration of the motor function across a variety of everyday tasks (Hughes et al. 1997; Rantanen et al. 1999; Francis and Spirduso 2000). All these tasks involve redundant sets of elements (muscles, digits, joints, limbs, etc.), which means that typical numbers of task constraints are smaller than the number of elements (the problem of motor redundancy, Bernstein 1967). There are two major approaches to the problem of motor redundancy. One of them assumes that the neural controller selects magnitudes of elemental variables that optimize (maximize or minimize) a certain cost function resulting in a single, optimal solution (reviewed in Nelson 1983; Prilutsky 2000). The other approach (principle of abundance, Gelfand and Latash 1998) assumes that the neural controller facilitates families of solutions that stabilize important performance variables; individual solutions emerge from these families by chance.

Within the first approach, several studies assumed that the central controller employed various cost functions and showed that motor performance by elderly persons leads to less optimal values of those functions as compared to the performance by younger persons (Cooke et al. 1989; Walker et al. 1997; Contreras-Vidal et al. 1998). In those studies, cost functions were assumed based on the intuition and experience of the researchers. Recently, a novel method has been introduced, analytical inverse optimization (ANIO, Terekhov et al. 2010) that allows to infer a cost function from experimental observations (certainly, under a number of assumptions). The method has been applied successfully to multifinger total force and moment of force, $\{F_{TOT}; M_{TOT}\}$, production tasks by young persons (Park et al. 2010). The first objective of this study has been to compare the cost functions reconstructed based on similar sets of accurate $\{F_{TOT}; M_{TOT}\}$ production tasks performed by elderly and young persons. We hypothesized that both young and elderly persons will use cost functions of the same analytical form, that is second-order polynomials with linear terms (as in Park et al. 2010, 2011). We expected, however, that the coefficients at different terms of the functions, that is, the costs of force production by individual fingers, will show consistent changes with age reflecting changes in the finger control.

Within the second approach, a quantitative method has been developed to quantify multidigit synergies in the framework of the uncontrolled manifold (UCM) hypothesis (Scholz and Schöner 1999; reviewed in Latash et al. 2002, 2007). The UCM hypothesis assumes that the neural controller acts in a space of elemental variables (individual finger forces in this study), and organizes within that space a sub-space (UCM) corresponding to desired values of potentially important performance variables ($\{F_{TOT}; M_{TOT}\}$ in this study). Further, the CNS tries to limit variance across repetitive attempts at the task in directions orthogonal to the UCM ("bad variance" or V_{ORT}) while it allows relatively large variance within the UCM ("good variance" or V_{UCM}). A single metric has been used to quantify such synergies reflecting the relative amount of V_{UCM} in the total variance, in particular in multidigit studies (Kang et al. 2004; Olafsdottir et al. 2005; Shim et al. 2005b; Gorniak et al. 2007, 2009). Several studies have documented lower synergy indices in elderly persons during multidigit pressing tasks with accurate F_{TOT} and M_{TOT} production (Shinohara et al. 2003a, b, 2004; Olafsdottir et al. 2007) and prehensile tasks with static holding a handle against a combination of external load and torque (Shim et al. 2004).

The two approaches, optimization and principle of abundance, seem incompatible because the former assumes that a single solution is generated while the latter assumes that families of solutions are always used. This contrast may, however, be only seeming. In a recent study (Park et al. 2010), we applied both methods, ANIO and UCM-based analysis, to $\{F_{TOT}; M_{TOT}\}$ production tasks by young persons. The results have suggested that an optimization principle could be used to select combinations of elemental variables (i.e., finger forces) that define sharing of the task among elemental variables, while synergies dictate patterns of finger force covariation across trials at the same task. We expected that using both methods will allow additional insights into the age-related changes in the neural control of the fingers.

Our second objective was to link age-related differences in the cost functions defined by the ANIO method to changes in the indices of multifinger synergies. Imagine a rather simple task of producing a required total force magnitude while pressing with two fingers on two force sensors (described in more detail in "Discussion" and illustrated in Fig. 8). This task has an infinite number of solutions. If a person is asked to perform it several times, a cloud of data points will be observed (e.g., Latash et al. 2001; Gorniak et al. 2007). The center of the cloud will define a preferred sharing of the total force between the two fingers (for example, 55:45%). The shape of the cloud will define the pattern of finger force covariation. In general, the location of the data cloud and its shape are independent.

In this study, we asked the subjects to perform two tasks with accurate production of $\{F_{TOT}; M_{TOT}\}$ combinations. One of them covered a broad range of $\{F_{TOT}; M_{TOT}\}$ values with just one trial per $\{F_{TOT}; M_{TOT}\}$ combination—to apply the ANIO method. The other task used only four $\{F_{TOT}; M_{TOT}\}$ combinations with multiple repetitions at each—to quantify multifinger synergies. We hypothesized that changes in characteristics of optimal performance defined across numerous tasks (sharing) would correlate

with age-related differences in synergy indices (co-variation) defined during repetitive trials at the same task.

Methods

Subjects

Seven healthy elderly subjects (five women and two men) and seven healthy young subjects (three women and four men) participated in the study. Their average age, height, and weight were 79.43 ± 4.31 years (mean ± standard deviation), 163.71 ± 7.70 cm, 62.68 ± 10.27 kg for the elderly subjects, and 29.86 ± 2.27 years, 171.29 ± 9.66 cm, 63.57 ± 10.08 kg for the young subjects. All subjects were right-handed as determined by the Edinburgh Handedness Inventory (Oldfield 1971). None of the subjects had a previous history of neuropathies or traumas to their upper extremities. The elderly subjects were recruited from a local retirement community. A screening test for the elderly subjects involved a cognition test (mini mental status exam ≥24 points), a depression test (Beck depression inventory ≤20 points), a quantitative sensory test (monofilaments ≤3.22), and a general neurological examination. Before testing, the experimental procedures of the study were explained and the subjects signed a consent form approved by the Office for Research Protection in the Pennsylvania State University.

Equipment

Four force sensors (Nano-17, ATI Industrial Automation, Garner, NC) were used to measure finger pressing forces (i.e., normal forces). The sensors were attached to a customized flat panel (140 × 90 × 5 mm) as shown in Fig. 1c. Each sensor was covered with sandpaper in order to increase the friction between subject's finger tips and the top surface of sensors. On the panel, there were four slots along the X-axis, which allowed attaching sensors and adjusting position of sensors according to the individual hand and finger lengths of each subject. The sensors were mediolaterally aligned 3.0 cm apart within the panel. The panel was mechanically fixed to a stationary table. The four normal force signals were digitized at 200 Hz with a 16-bit resolution (PCI-6225, National Instrument, Austin, TX) with a customized LabVIEW program (LabVIEW 8.5, National Instrument, Austin, TX). Matlab (Matlab 7.4.0, Mathworks, Inc) programs were written for data processing and analysis.

Experimental procedures

Before the experiment, subjects had a 30 min orientation session to become familiar with the experimental setup,

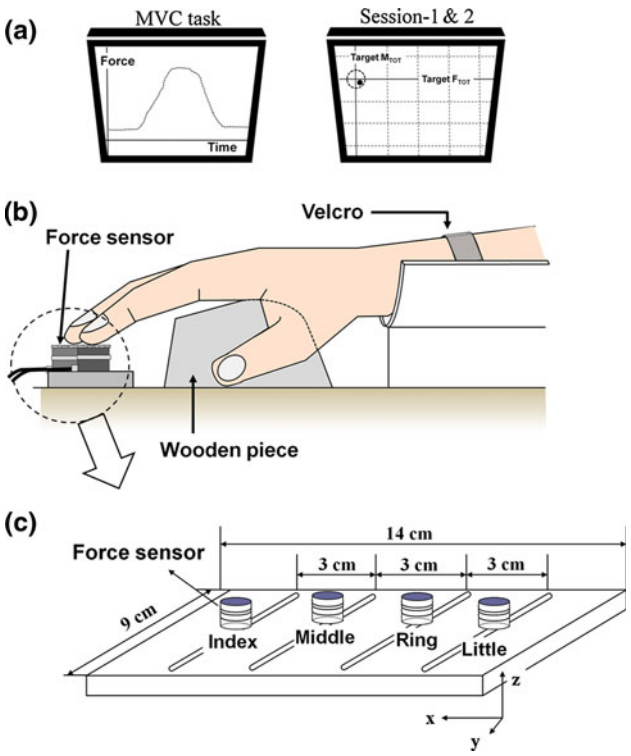

Fig. 1 **a** The feedback screens during the MVC task and accurate force-moment production tasks (session-1 and session-2). During session-1 and session-2, the produced F_{TOT} and M_{TOT} values were displayed on the computer screen with the cursor showing F_{TOT} along the vertical axis and M_{TOT} along the horizontal axis. **b** The experimental setup. A wooden piece, which supported the subject's right palm, was used to ensure a constant configuration of the hand and fingers. **c** The finger pressing setup. The sensors, shown as *white cylinders*, were attached to a wooden frame. The frame was fixed to the immovable table

and to ensure that they were able to perform the tasks. The subjects sat in a chair facing the 19-inch computer screen and positioned their right upper arm on a wrist-forearm brace that was fixed to the table. The forearm was held stationary with Velcro straps to prevent forearm and wrist movement. A wooden piece, which supported the subject's right palm, was used to ensure a constant configuration of the hand and fingers (Fig. 1b). Similar setups were used in earlier studies (Li et al. 1998; Kang et al. 2004; Olafsdottir et al. 2007); they allow avoiding changes in the hand/finger configuration without compromising subject's comfort. Prior to each trial, the subjects were asked to place their fingertips on the sensor centers and then all signals were set to zero. The experiment consisted of maximal voluntary contraction (MVC) tasks and accurate force–moment production tasks.

MVC tasks were performed by the index finger alone (MVC_I) and by all four fingers pressing together (MVC_{IMRL}). The subjects were instructed to reach maximal force within 3 s. The maximal force was measured and

used to determine the target force and moment magnitudes in the next force–moment production tasks. During the MVC_I task, the subjects were asked to keep all the fingers on the sensors and ignore possible force production by other fingers. For each MVC task, the subject performed three consecutive attempts, and the average MVC_{IMRL} and MVC_I over the three attempts were computed.

There were two sessions with accurate force–moment production tasks. These tasks required the subjects to produce various combinations of steady-state levels of total normal force (F_{TOT}) and moment of normal force (M_{TOT}; computed from the normal force values with respect to the midpoint between the middle and ring fingers) as accurately as possible. Note that computing M_{TOT} based on assumed lever arm values for individual fingers allowed to avoid effects of small changes in the actual lever arms with changes in the point of finger force application. The produced F_{TOT} and M_{TOT} values were displayed on the computer screen with the cursor showing F_{TOT} along the vertical axis and M_{TOT} along the horizontal axis (Fig. 1a). During each trial, the subjects were given 6 s to reach the target values of F_{TOT} and M_{TOT} as accurately as possible and maintain these values for at least 1.5 s. Real-time feedback on F_{TOT} and M_{TOT} was provided on a 19-inch monitor screen positioned 0.5 m in front of the subject.

In the first force–moment production session, the F_{TOT} levels included 20, 25, 30, 35, 40, 45, 50, 55, and 60% (9 levels) of MVC_{IMRL}. The M_{TOT} levels included 2.0PR, 1.5PR, 1.0PR, 0.5PR, 0PR, 0.5SU, 1.0SU, 1.5SU, and 2SU (9 levels); PR—pronation, SU—supination. 1PR was defined as the product of 7% of MVC_I by the lever arm of the index finger ($d_i = -4.5$ cm). These F_{TOT} and M_{TOT} levels were chosen to cover a broad range of $\{F_{TOT}; M_{TOT}\}$ combinations without producing fatigue. The subjects performed one trial for each $\{F_{TOT}; M_{TOT}\}$ combination in a random order for a total of 81 trials.

In the second force-moment production session, there were two F_{TOT} levels (20 and 40% of MVC_{IMRL}) and two M_{TOT} levels (2PR and 2SU). Each subject performed 20 trials for each of the four conditions for a total of 80 trials. The purpose of collecting multiple trials in session-2 was to be able to apply the uncontrolled manifold analysis of the finger force variance. After each trial, a 20 s break was given to avoid finger fatigue. When the subjects requested, additional rest was provided. The order of F_{TOT}, M_{TOT} combinations was randomized in each session. The entire experiment lasted approximately 1.5 h.

Note that M_{TOT} in this study, represents a linear function of normal finger forces, not the actual moment of force. In particular, possible shifts of finger force application points on the sensor surface and moments produced by shear forces were not considered.

Data analysis

Initial data processing

The force data were digitally low-pass filtered with zero-lag, 4th-order Butterworth filter at 5 Hz. Further, the data from each trial were averaged over 1.5 s in the middle of the time period where steady-state values of force and moment were observed (identified by visual data inspection). These averaged values were used for further analysis.

Each task involved two constraints:

$$F_{TOT} = F_i + F_m + F_r + F_l = \alpha \cdot MVC_{IMRL} \quad (1)$$

where the subscripts *i, m, r,* and *l* stand for the index, middle, ring and little fingers, respectively, and α indicates a given percentage of MVC (for session-1, $\alpha = 20$, 25, 30, 35, 40, 45, 50, 55, and 60%; for session-2, $\alpha = 20$ and 40%).

$$\begin{aligned} M_{TOT} &= d_i \cdot F_i + d_m \cdot F_m + d_r \cdot F_r + d_l \cdot F_l \\ &= \beta \cdot 0.07 \cdot d_i \cdot MVC_I = \beta \cdot 1PR \end{aligned} \quad (2)$$

where d stands for the lever arm. We assumed that the lever arms (d_i, d_m, d_r, and d_l) were constant with respect to the mid-point between the middle and ring fingers: $d_i = -4.5$ cm, $d_m = -1.5$ cm, $d_r = 1.5$ cm, and $d_l = 4.5$ cm in the mediolateral direction. Thus, $\beta = -2, -1.5, -1, -0.5$, 0, 0.5, 1, 1.5, and 2 for session-1, and $\beta = -2$ and 2 for session-2.

The ANIO approach

First, principal component analysis (PCA) was performed on the finger force data in all the trials in session-1 performed by each subjects separately (81 data points). The Kaiser Criterion (Kaiser 1960) was employed to extract the significant PCs (those with eigenvalues over 1.0), and the percent of the total variance explained by the first two PCs was computed in order to check planarity of the data point distributions. For the computational details of the ANIO approach, see Appendix 1. The objective function was assumed to be:

$$J = \frac{1}{2}\sum_i k_i (F_i)^2 + \sum_i (w_i) F_i \quad (3)$$

where $i = \{$index, middle, ring, and little$\}$; k and w are coefficients, and k_{index} was set at 1 in order to normalize the coefficients for across subjects comparisons. The second-order terms were expected to be all positive to comply with assumptions of the objective function minimization (Terekhov et al. 2010); this was indeed true (see "Results"). Based on the computed function J, a plane of optimal solutions was computed for the $\{F_{TOT}; M_{TOT}\}$ combinations used in the experiment. The angle between

the plane of optimal solutions and the plane determined by the experimental observations was computed (D-angle).

Co-contraction index

The IM and RL finger pairs produced moments in opposite directions. For each task, the moment produced by the pair acting in the required direction (agonist moment, M_{AGO}) and against the required direction (antagonist moment, M_{ANT}) were computed. Further, a co-contraction index (CCI) was computed as:

$$CCI = 1 - \frac{|M_{AGO}| - |M_{ANT}|}{|M_{AGO}| + |M_{ANT}|} = 2\frac{|M_{ANT}|}{|M_{AGO}| + |M_{ANT}|} \quad (4)$$

Theoretically, CCI could range from 0 ($M_{ANT} = 0$), to 1 ($M_{AGO} = -M_{ANT}$).

Moment of force sharing analysis

The *I* and *L* (lateral) fingers had larger moment arms with respect to the nominal pivot as compared to the *M* and *R* (central) fingers, 4.5 cm versus 1.5 cm. To estimate the share of the moment of force produced by the lateral fingers, we computed the percent of the total moment of force in the required direction (agonist moment, M_{AGO}) and against the required direction (antagonist moment, M_{ANT}). For PR tasks, *I* and *M* fingers produced M_{AGO} while *R* and *L* fingers produced M_{ANT}. For SU tasks, *R* and *L* fingers produced M_{AGO} while *I* and *M* fingers produced M_{ANT}. The following indices were computed reflecting the percent of the total moment produced by the lateral finger within each of the two finger pairs (IM and RL) when they acted as agonists and as antagonists:

$$\%M_{AGO\_Lateral} = \frac{M_{AGO\_Lateral}}{M_{AGO}} \times 100 \quad (5)$$

$$\%M_{ANT\_Lateral} = \frac{M_{ANT\_Lateral}}{M_{ANT}} \times 100. \quad (6)$$

Analysis of finger force covariation

The force data were analyzed within the framework of the uncontrolled manifold (UCM) hypothesis (Scholz and Schöner 1999). The hypothesis offers a method to compute the extent to which the values of relevant performance variables (F_{TOT} and M_{TOT}) are stabilized by the covariation of individual finger forces across trials at the same task. The data from session-2 were used to compute two components of finger force variances across 20 trials. One of the components (V_{UCM}) reflected force variance that did not change the averaged across trials magnitude of the selected performance variable, while the other component (V_{ORT}) reflected force variance that did. V_{UCM} and V_{ORT} were computed with respect to F_{TOT}, M_{TOT}, and $\{F_{TOT}, M_{TOT}\}$ simultaneously as performance variables. The computational details are presented in Appendix 2. Further, an index reflecting the relative amounts of V_{UCM} and V_{ORT} was computed as:

$$\Delta V = \frac{V_{UCM} - V_{ORT}}{V_{TOT}} \quad (7)$$

where V_{TOT} stands for the total finger force variance, and each variance index is computed per degree-of-freedom in the corresponding spaces. ΔV was computed with respect to F_{TOT} (ΔV_F), M_{TOT} (ΔV_M), and $\{F_{TOT}, M_{TOT}\}$ (ΔV_{FM}). Prior to statistical analysis (see later), this index was transformed using a Fisher *z*-transformation (ΔV_z) adapted to the boundaries of ΔV. The angle between the UCM and the optimal plane computed using the ANIO method was calculated in the four-dimensional finger force space. We will refer to this angle as the UCM-optimal angle.

Statistics

The data are presented as means and standard errors.

For the data from session-1, we explored whether the two groups (young and elderly) differed in the amount of variance explained by the first two PCs, in the loadings of each of the first two PCs (i.e., each PC was analyzed separately), in the coefficients (k_i and w_i) in the *J* function, in the D-angle between the planes of optimal solutions and experimental observations, in the co-contraction index (CCI), and in the torque shares produced by the lateral moment agonist ($\%M_{AGO\ Lateral}$) and moment antagonist ($\%M_{ANT\ Lateral}$) fingers. Prior to ANOVAs, variables with computational boundaries were transformed using a Fisher's *z*-transformation adapted to the boundaries.

For the data from session-2, mixed-design ANOVAs with repeated measures were used. In particular, we explored how variance within the two subspaces (factor *Variance* with two levels, V_{UCM} and V_{ORT}) were affected by *Age* and by other factors such as *Force* (20 and 40% of MVC_{IMRL}) and *Moment* (2SU and 2PR). Analyses were run separately for each of the three performance variable, F_{TOT}, M_{TOT} and $\{F_{TOT}; M_{TOT}\}$. ANOVA with repeated measures was also performed on the *z*-transformed ΔV index. Factors for particular comparisons will be described in more detail in the "Results" section. Tukey's honestly significant difference tests and pairwise contrasts were used to explore significant effects.

Multiple regression models were used to determine whether the index of stabilizations of performance variables from session-2 (ΔV_F, ΔV_M, and ΔV_{FM}) could be predicted from a subset of variables computed based on session-1. The multiple regression models used the percent of total variance explained by the first two PCs and the

D-angle computed based on the cost function J as predictors. Dependent variables were ΔV_F, ΔV_M, and ΔV_{FM} from session-2. The UCM-optimal angle was computed and compared between the two groups and also to 90° (t-tests). The level of significance was set at $P < 0.05$.

Results

Principal component (PC) analysis

The principal component analysis (PCA) was performed on the sets of 81 observations in session-1, which covered a broad range of $\{F_{TOT}; M_{TOT}\}$ combinations. The first two PCs accounted for more than 90% of the total variance in the finger force space for the young group. For the elderly group, the first two PCs accounted for only about 75% of the total variance (Table 1). These results imply that that the experimental observations in the young group were confined to a two-dimensional hyperplane in the four-dimensional force space, while the experimental observations in the elderly were not. The amount of variance explained by PC1 for the elderly was around 46%, much smaller than for the young (70%). In contrast, the amount of variance explained by PC2 for the elderly (30%) was larger than that for the young (22%).

For both groups, all four finger forces had large loadings with the same sign (i.e., positive loadings) in PC1 (Fig. 2a). In PC2, the loadings of the I and M finger forces were of the same sign, while the signs of the loadings for the R and L finger forces were opposite (Fig. 2b). There was significant difference between the young and elderly groups in the loading magnitudes. In PC1, the loadings of the M and R finger forces in the young group were larger than those of the I and L finger forces, which was not true in the elderly group (Fig. 2a). In PC2, there was a pattern of loading factor absolute magnitudes in the young group, $I > M$, $L > R$, which was not observed in the elderly group (Fig. 2b).

These findings were supported by two-way repeated measure ANOVAs on z-transformed PC loadings with factors *Finger* (I, M, R, L) and *Age* (young and elderly). Both main effects were statistically significant for both PC1 and PC2 loadings [*Finger*: $F_{[3,36]} = 8.94$, $P < 0.001$ for PC1; $F_{[3,36]} = 55.20$, $P < 0.001$ for PC2] and [*Age*: $F_{[1,12]} = 22.73$, $P < 0.001$ for PC1; $F_{[1,12]} = 11.69$, $P < 0.01$ for PC2] with a significant interaction *Age* × *Finger*: $F_{[3,36]} = 8.65$, $P < 0.001$ for PC1; $F_{[3,36]} = 5.02$, $P < 0.01$ for PC2. The *Age* × *Finger* interaction reflected that in PC1, the difference between the age groups was observed for the M and R loading values (young > elderly) while for PC2, this was true for the M loading values (young > elderly). In PC1, the loading values for M and R were larger than for I for the young group, while the loading values for R and L were larger than for M for the elderly group. For PC2, the loading values for R and L were larger than those for I and M for both groups. The absolute values of the loadings for the young group were higher for

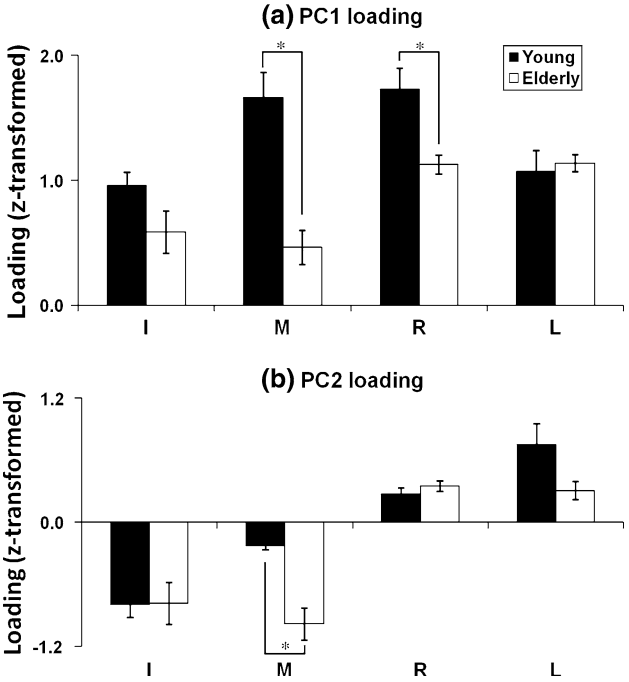

Fig. 2 Loading factors of PC1 (**a**) and PC2 (**b**) of individual finger forces for the young (*black bars*) and elderly (*white bars*) from session-1. The data for the second-order coefficient for the index finger (k_I) are not presented because k_I was set at 1 in order to normalize the rest of the coefficients. The average z-transformed PC loadings of individual finger forces across subjects are presented with standard *error bars*. I, M, R, and L indicate index, middle, ring, and little fingers, respectively. The *asterisks* show statistically significant differences between age groups ($P < 0.05$)

Table 1 Variance explained by PCs

	PC1		PC2		PC1 + PC2	
	Mean	Range [min, max]	Mean	Range [min, max]	Mean	Range [min, max]
Young	69.82	[58.85, 86.73]	21.34	[11.31, 26.93]	91.16	[82.06, 98.04]
Elderly	46.71	[41.17, 52.74]	30.04	[26.01, 36.35]	76.75	[71.11, 86.62]

The average and minimal–maximal percent variances (in parentheses) explained by PC1, PC2, and PC1 + PC2 across subjects are shown

the "lateral" fingers with larger lever arms (*I* and *L*) as compared to the "central" fingers with smaller lever arms (*M* and *R*) only in the young group. All these findings were supported by pairwise comparisons ($P < 0.05$).

The ANIO approach

Based on the results of the PCA analysis, we assumed that the cost function represented a second-order polynomial, $J = \frac{1}{2}\sum_i k_i(F_i)^2 + \sum_i (w_i)F_i$ (see Methods and Terekhov et al. 2010). Further, we determined the coefficients at the quadratic (k_i) and the linear terms (w_i) to provide best fit to the data. These coefficients for individual subjects are presented in Table 2. The coefficients at the second-order terms were positive for all subjects. This finding supports the assumption of *J* minimization (see Appendix 1).

Figure 3 shows the average *k* and *w* coefficients across subjects for each of the two groups. The second-order coefficient for the index finger force (k_I) is not included because its value was set at 1 in order to normalize the rest of the coefficients. The second-order coefficients within the young group were larger than those in the elderly group, while there was no significant difference in the first-order coefficients between two age groups. This finding was supported by two-way repeated measure ANOVAs with factors *Finger* (three levels: *M*, *R*, *L* for *k*; four levels: *I*, *M*, *R*, *L* for *w*) and *Age*. The main effect of *Finger* was statistically significant for both *k* and *w* [$F_{[2,24]} = 9.26$, $P < 0.01$ for *w*; $F_{[3,36]} = 46.14$, $P < 0.001$ for *k*], while the main effect of *Age* was significant only for *k* [$F_{[1,12]} = 14.31$, $P < 0.01$]. There were no significant interactions. The pairwise comparisons confirmed that k_L was larger than k_M and k_R ($P < 0.01$). All pairwise comparisons on *w* were significant ($P < 0.01$).

The D-angle was computed between the plane of optimal solutions and the plane containing the experimental observations (see "Methods"). On average, the angle was smaller in the young group (1.38° ± 0.80°) as compared to the elderly group (5.10° ± 1.07°). This difference was significant according to the *t*-test ($P < 0.05$).

Co-contraction index

Across all conditions with non-zero moment (*M*) production, fingers that acted against the required direction of *M* produced non-zero forces. These forces contributed to the antagonist moment of force (M_{ANT}). The co-contraction index (CCI) was computed to reflect the relative magnitude of M_{ANT} with respect to the moment produced by fingers acting in the required direction (agonist moment, M_{AGO}; see Eq. 4 in "Methods"). Overall, CCI in the elderly group was smaller than that in the young group, and CCI increased with the magnitude of prescribed forces (Fig. 4). In addition, CCI was larger for smaller magnitudes of prescribed moment of force with no clear differences between moment in pronation (PR) and supination (SU).

A three-way repeated measures ANOVA was performed on the CCI with factors *Age*, *Force* (Low, Mid, and High), and *Moment* (PR_{HIGH}, PR_{LOW}, SU_{LOW}, and SU_{HIGH}). For this analysis, task forces were grouped into Low, Mid, and High forces covering 20–30%, 35–45%, and 50–60% of MVC_{IMRL}, respectively. Task moments were grouped into PR_{HIGH}, PR_{LOW}, SU_{LOW}, and SU_{HIGH} that included {2.0PR, 1.5PR}, {1.0PR, 0.5PR}, {0.5SU, 1.0SU}, and

Table 2 The estimation of parameters k_i and w_i from the ANIO approach

		k_{index}	k_{middle}	k_{ring}	k_{little}	w_{index}	w_{middle}	w_{ring}	w_{little}	D-angle (°)
Young	s01	1.00	0.62	0.73	0.88	−0.39	0.43	0.32	−0.36	0.09
	s02	1.00	0.53	0.48	0.41	−0.11	0.27	−0.19	0.04	0.72
	s03	1.00	0.39	0.65	0.88	−1.05	1.34	0.47	−0.76	0.21
	s04	1.00	0.42	0.48	0.59	−0.28	0.54	−0.23	−0.03	0.28
	s05	1.00	0.14	0.11	0.20	−0.48	0.58	0.27	−0.37	1.71
	s06	1.00	0.23	0.44	0.99	−0.57	0.67	0.36	−0.46	6.34
	s07	1.00	0.19	0.09	0.13	−0.49	0.61	0.26	−0.38	0.32
Elderly	s08	1.00	0.04	0.10	0.54	−0.18	0.19	0.16	−0.17	1.05
	s09	1.00	0.02	0.06	0.15	−0.65	0.73	0.48	−0.56	5.84
	s10	1.00	0.02	0.03	0.16	−0.49	0.63	0.21	−0.35	2.17
	s11	1.00	0.02	0.02	0.13	−0.51	0.62	0.30	−0.40	4.01
	s12	1.00	0.001	0.001	0.004	−0.38	0.51	0.13	−0.26	6.22
	s13	1.00	0.10	0.07	0.52	−0.77	0.95	0.42	−0.60	7.69
	s14	1.00	0.02	0.02	0.09	−0.44	0.58	0.17	−0.30	8.74

* k_i and w_i are the second-order and first-order coefficients, respectively. D-angle is the angle between the plane of experimental observations and the plane of optimal solutions computed based on the cost function

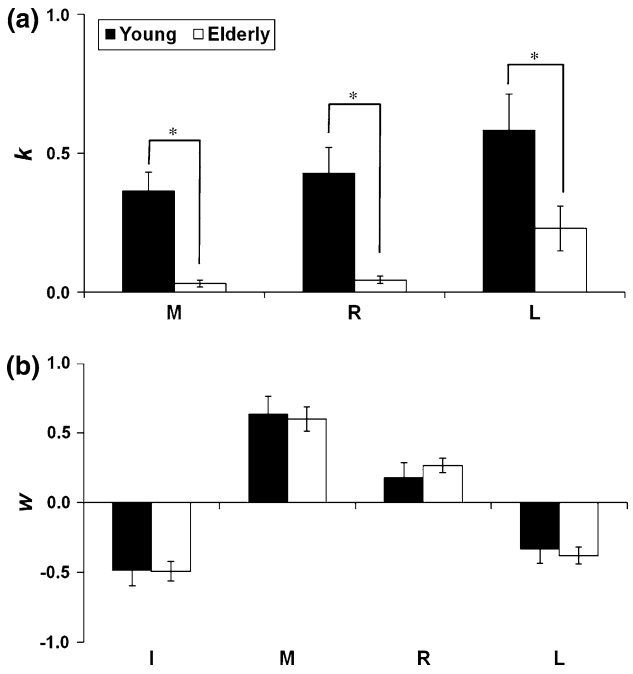

Fig. 3 **a** The coefficients of the second-order terms (k) and **b** of the first-order terms (w) within the cost functions computed using the ANIO method for the young (*black bars*) and elderly (*white bars*) groups. The average values across subjects are presented with standard *error bars*. I, M, R, and L indicate index, middle, ring, and little fingers, respectively. The *asterisks* show statistically significant differences between the age groups ($P < 0.05$)

{1.5SU, 2.0SU}, respectively. Zero PR (SU) condition was excluded. The three main effects were statistically significant [*Age*: $F_{[1,12]} = 19.85$, $P < 0.001$; *Force*: $F_{[2,24]} = 274.184$, $P < 0.001$; and *Moment*: $F_{[3,36]} = 151.63$, $P < 0.001$] without significant interaction. Pairwise comparisons showed significant differences of the CCI among levels of forces ($CCI_{Low\ force} < CCI_{Mid\ force} < CCI_{High\ force}$) and moments ($CCI_{PR\text{-}HIGH}$, $CCI_{SU\text{-}HIGH} < CCI_{PR\text{-}LOW}$, $CCI_{SU\text{-}LOW}$) ($P < 0.01$).

Analysis of moment of force sharing

To explore whether the different loading patterns in PC2 in the two groups (Fig. 2b) reflected different involvement of individual fingers in the moment of force production, the percent of the agonist and antagonist moment of force produced by the lateral agonist fingers ($\%M_{AGO\_Lateral}$ and $\%M_{ANT\_Lateral}$) with respect to the total M_{AGO} and M_{ANT} was computed (see Eq. 5 and 6 in Methods). Figure 5 shows these indices for the different force levels (Low, Middle, and High) and different moment levels (PR and SU, high and low). Both indices were significantly larger in the young group (black columns, on average close to 70%) as compared to the elderly group (white columns, on average about 50%). Figure 5a shows also that $\%M_{AGO\_Lateral}$ decreased with the magnitude of prescribed forces, particularly for large magnitudes of the moment of force (i.e., for PR_{HIGH} and SU_{HIGH}). No such differences are seen for $\%M_{ANT\_Lateral}$ (Fig. 5b).

Three-way repeated measures ANOVAs were performed on both $\%M_{AGO\_Lateral}$ and $\%M_{ANT\_Lateral}$ with factors *Age*, *Force* (Low, Middle, and High), and *Moment* (PR_{HIGH}, PR_{LOW}, SU_{LOW}, and SU_{HIGH}). All three main effects were significant for $\%M_{AGO\_Lateral}$ [*Age*: $F_{[1,12]} = 11.00$, $P < 0.01$; *Force*: $F_{[2,24]} = 26.62$, $P < 0.001$; and *Moment*: $F_{[3,36]} = 9.61$, $P < 0.001$] with a significant *Force* × *Moment* interaction [$F_{[6,72]} = 4.34$, $P < 0.01$]. The interaction reflected the fact that $\%M_{AGO\_Lateral}$ at low forces was larger than that at the higher forces for high values of the moment (PR_{HIGH} and SU_{HIGH}), while this index was larger for larger moment of force magnitudes (PR_{HIGH} and $SU_{HIGH} > PR_{LOW}$ and SU_{LOW}) at lower forces ($P < 0.05$). ANOVA on $\%M_{ANT\_Lateral}$ showed only the main effect of

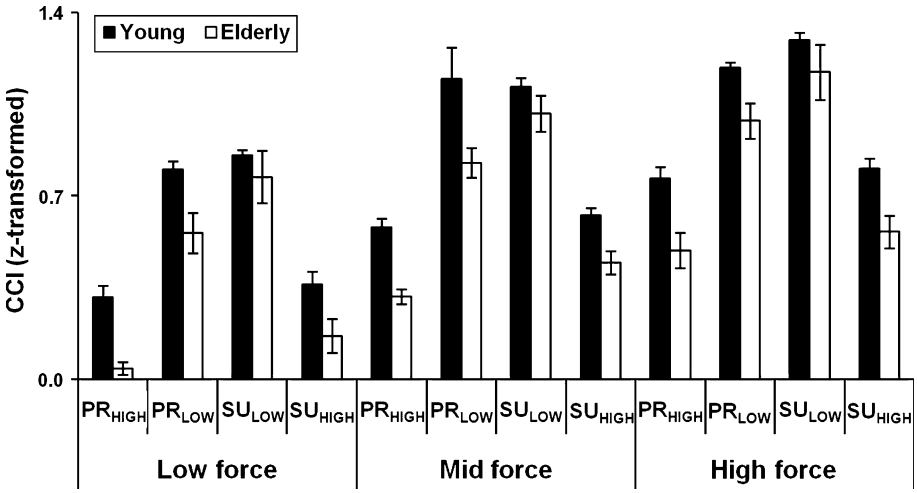

Fig. 4 *Z*-transformed co-contraction index (CCI) for different {F_{TOT}; M_{TOT}} combinations for the young (*black bars*) and elderly (*white bars*) groups. The average values across subjects are presented with standard *error bars*. Low, Mid, and High forces correspond to the ranges of 20–30%, 35–45%, and 50–60% of MVC_{IMRL}, respectively. PR_{HIGH}, PR_{LOW}, SU_{LOW}, and SU_{HIGH} correspond to the ranges {2.0PR, 1.5PR}, {1.0PR, 0.5PR}, {0.5SU, 1.0SU}, and {1.5SU, 2.0SU}, respectively

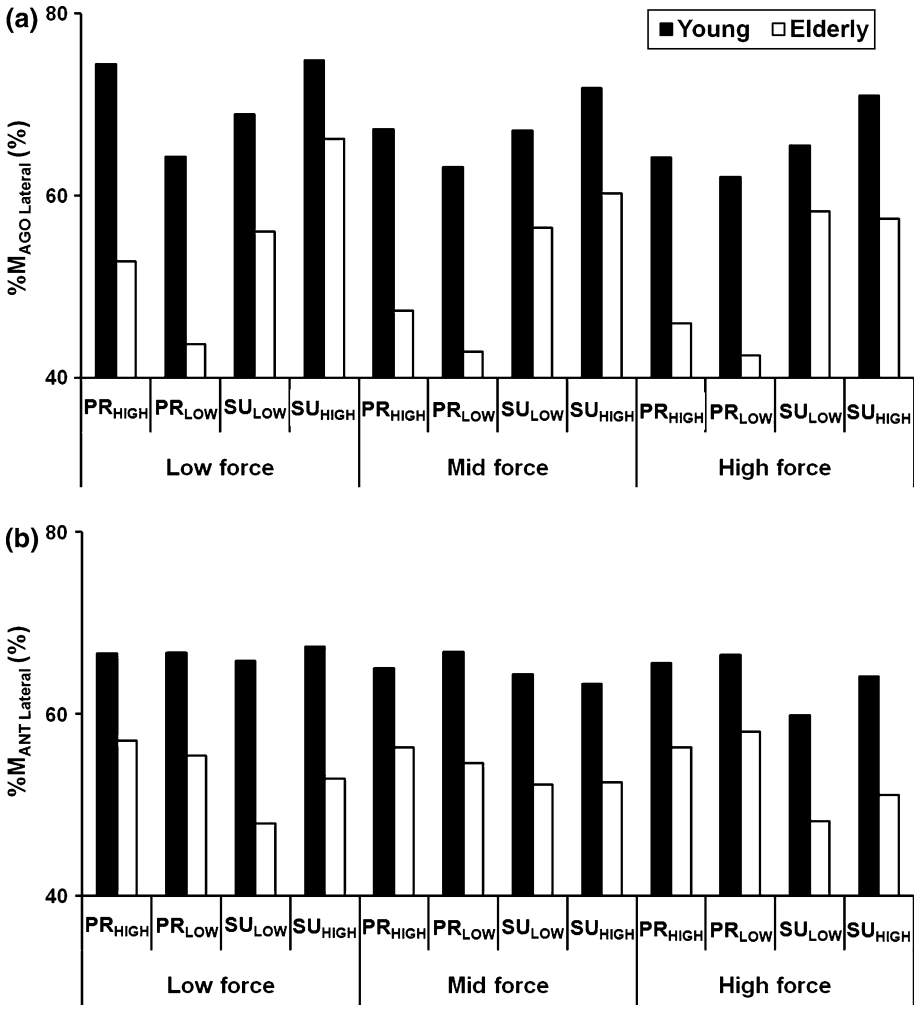

Fig. 5 **a** The percent torque produced by lateral agonist ($\%M_{AGO\_Lateral}$) to total agonist moment (M_{AGO}) and **b** the percent torque produced by lateral antagonist ($\%M_{ANT\_Lateral}$) to the total antagonist moment (M_{ANT}) for the young (*black bars*) and elderly (*white bars*) groups. The average values across subjects are presented. Low, Mid, and High forces correspond to the ranges of 20–30%, 35–45%, and 50–60% of MVC_{IMRL}, respectively. PR_{HIGH}, PR_{LOW}, SU_{LOW}, and SU_{HIGH} correspond to the ranges {2.0PR, 1.5PR}, {1.0PR, 0.5PR}, {0.5SU, 1.0SU}, and {1.5SU, 2.0SU}, respectively

Age [$F_{[1,12]} = 6.50$, $P < 0.05$] without other effects or interactions.

The UCM analysis

Multifinger synergies stabilizing total force (F_{TOT}), moment (M_{TOT}), and force and moment simultaneously ({F_{TOT}; M_{TOT}}) were quantified within the framework of the UCM hypothesis. Two components of finger force variance, V_{UCM} and V_{ORT}, were computed per degree-of-freedom using experimental observations in session-2 (see "Methods"). Pilot analyses showed no effects of *Moment* on variance indices. Hence, the factor *Moment* was excluded in the rest of statistical analysis for this section.

Overall, V_{UCM} was always greater than V_{ORT} (Fig. 6). V_{UCM} increased with the magnitude of prescribed force across all subjects and conditions. Both V_{UCM} and V_{ORT} were smaller in the young group as compared to the elderly group, especially for the higher force level (40% of MVC_{IMRL}). These results were supported by an ANOVA on variance indices that showed significant main effects of *Variance* (V_{UCM} and V_{ORT}), *Force* (20 and 40% of MVC_{IMRL}), and *Age* (two levels: the young and elderly) for all three analyses (Table 3).

The significant interactions *Variance* × *Force* reflected the fact that V_{ORT} did not increase with force magnitude while V_{UCM} did for both groups. The *Age* × *Force* interaction reflected the fact that both V_{UCM} and V_{ORT} in the elderly group were larger than in the young group, but only for the force level of 40% of MVC_{IMRL} ($P < 0.01$).

The ΔV indices related to F_{TOT} (ΔV_F), M_{TOT} (ΔV_M), and {F_{TOT}, M_{TOT}} (ΔV_{FM}) were quantified as the normalized difference between V_{UCM} and V_{ORT} (see "Methods"; Fig. 7). In general, $\Delta V_M > \Delta V_F > \Delta V_{FM}$ for both age groups and across the experimental conditions. The ΔV indices for the young group were larger than that for the elderly group for the high force (40% MVC) tasks. A three-way repeated measures ANOVA with the factors *Force*, *Age*, and *Analysis* (F_{TOT}-related, M_{TOT}-related, and {F_{TOT};M_{TOT}}-related) was performed on *z*-transformed ΔV values. The main effects of *Age* ($F_{[1,7]} = 36.02$, $P < 0.0001$) and *Analysis* ($F_{[2,14]} = 27.86$, $P < 0.001$)

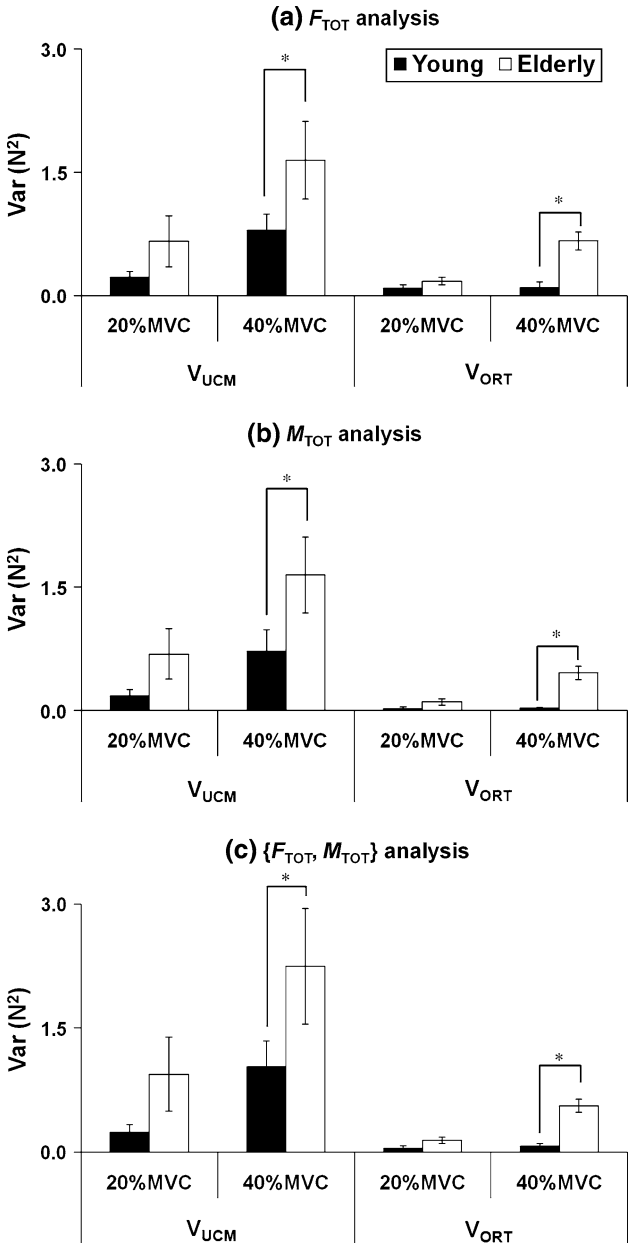

Fig. 6 Two components of variance, V_{UCM} and V_{ORT}, in the finger force space computed with respect to F_{TOT} (**a**), M_{TOT} (**b**), and {F_{TOT}; M_{TOT}} (**c**) as performance variables for the 20 and 40% of MVC_{IMRL} conditions for the young (*black bars*) and elderly (*white bars*) groups. Variances were normalized by degree-of-freedom of corresponding spaces. The average values (N^2) across subjects are presented with standard *error bars*. The *asterisks* show statistically significant differences between the age groups ($P < 0.05$)

were significant without a significant interaction. In addition, there was a significant *Age* × *Force* interaction ($F_{[1,7]} = 36.02$, $P < 0.001$). The interaction reflected the fact that ΔV for the young group increased with the force magnitude, while ΔV for the elderly group did not. The pairwise comparisons confirmed that $\Delta V_M > \Delta V_F > \Delta V_{FM}$ at all levels of *Age* and *Force* ($P < 0.01$).

The comparison between the UCM and ANIO analyses

The angle between two subspaces, the UCM and the space of optimal solutions defined with the ANIO approach was computed. Note that this UCM-optimal angle is different from the D-angle described earlier. The average UCM-optimal angle between the two planes across subjects in the young group was 78.55° ± 2.95°, significantly higher than in the elderly group, 57.26° ± 2.12° ($P < 0.05$). Both values were significantly smaller than 90° (*t*-tests; $P < 0.01$).

Multiple linear regression models were used to determine whether the synergy index ΔV computed based on the data within session-2 could be predicted based on a subset of outcome variables computed based on the data collected in session-1. The model used %PCs (the percent of total variance explained by the first two PCs) and D-angle (angle between the plane of optimal solutions and the plane of the experimental observations) as predictors, and ΔV_F, ΔV_M, and ΔV_{FM} computed for the 20 and 40% of MVC_{IMRL} conditions (and both moment conditions) as dependent variables. Note that the data of the two age groups ($n = 14$) overlapped, and hence were used together in the regression models.

The models showed that both %PC and D-angle were significant predictors of the synergy indices but only for the high-force conditions, 40%MVC [$F_{[2,11]} = 9.22$, $P < 0.01$ for ΔV_F; $F_{[2,11]} = 5.10$, $P < 0.05$ for ΔV_M; $F_{[2,11]} = 11.73$, $P < 0.01$ for ΔV_{FM}]. For those conditions, the models accounted for 62.6, 48.1, and 68.1% of variance in ΔV_F, ΔV_M, and ΔV_{FM}, respectively. Both D-angle (standardized coefficient $\beta = -0.37$, $P < 0.05$) and %PCs (standardized coefficient $\beta = 0.66$, $P < 0.05$) were significant predictors of ΔV_{FM} and ΔV_F. No significant effects were observed for the low-force conditions, 20% MVC.

Discussion

This is the first study to address effects of aging on two contrasting features of performance of multielement redundant motor systems: Optimality of performance and synergies stabilizing performance variables. Our results suggest that optimality and synergies are two aspects of a single problem of sharing a task in an optimal way among a set of effectors, and making sure that performance is stable across repetitions (see Park et al. 2010). Further, we discuss issues related to aging effects on both optimality of performance and multidigit synergies.

Optimality of multidigit performance

The ANIO method allows to estimate a cost function based on a set of experimental observations. However, it does not

Table 3 Summary of ANOVAs on variance indices

	F_{TOT} analysis		M_{TOT} analysis		$\{F_{TOT}, M_{TOT}\}$ analysis	
	F-value	*P*	*F*-value	*P*	*F*-value	*P*
Main effect						
Variance	$8.35_{[1,7]}$	<0.05	$13.29_{[1,7]}$	<0.001	$9.49_{[1,7]}$	<0.05
Force	$53.70_{[1,7]}$	<0.0001	$56.08_{[1,7]}$	<0.0001	$36.79_{[1,7]}$	<0.0001
Age	$4.76_{[1,7]}$	<0.05	$5.46_{[1,7]}$	<0.05	$4.82_{[1,7]}$	<0.05
Interaction						
Variance × force	$11.27_{[1,7]}$	<0.01	$21.11_{[1,7]}$	<0.01	$13.56_{[1,7]}$	<0.01
Age × force	$10.02_{[1,7]}$	<0.01	$9.65_{[1,7]}$	<0.01	$4.76_{[1,7]}$	<0.05

F-values are presented with degrees-of-freedom in brackets for the three-way ANOVAs with the factors *variance*, *force*, and *age*

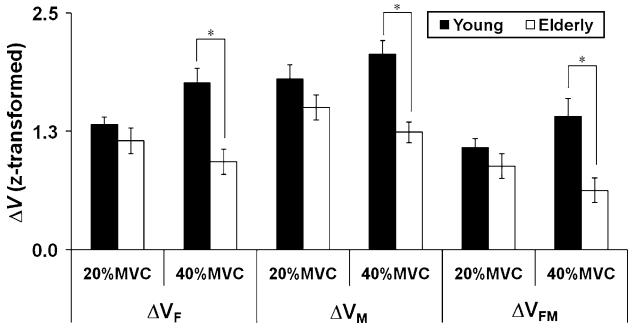

Fig. 7 *Z*-transformed ΔV (dimensionless) for the F_{TOT}-related (ΔV_F), M_{TOT}-related (ΔV_M), and $\{F_{TOT}, M_{TOT}\}$-related (ΔV_{FM}) analyses. *Black and white bars* represent ΔV for the young and elderly groups, respectively. Average ΔV_Z across subjects are presented with standard *error bars*. The *asterisks* show statistically significant differences between the age groups ($P < 0.05$)

ensure that the computed function is the "true one"; it is one from a possible set of functions that are able to describe the data with sufficient accuracy. An increase in the number of data points and in consistency of performance by the subject helps narrow such a set of possible cost functions, but never to a single one. There is no perfect criterion for how much variance should be accounted for by a subset of principal components that allow assuming a functional form *J*. That is why, after a cost function is defined, we used direct optimization to quantify the angle (D-angle) between the set of data points observed in the experiment (experimental plane) and a set of points computed for the same constraints based on the computed cost function (plane of optimal solutions). If the D-angle is small, one may conclude that the cost function reflects an unknown optimization principle with sufficient accuracy (see Terekhov et al. 2010).

It is well known that elderly persons show increased variability across a variety of motor tasks including accurate force production tasks (Cole et al. 1999; Burnett et al. 2000; Enoka et al. 2003; Shinohara et al. 2003a, b, 2004). In our experiment, this was reflected, in particular, in distributions of data points that deviated from a perfect plane significantly more than in young subjects. It was also reflected in the significantly higher "bad variability" (V_{ORT}) in the analysis of the data collected in session-2. The fact that the first two PCs accounted for only about 75% of variance in the elderly group (in contrast to >90% in the young group) may reflect two factors. First, the data distributions could be significantly non-planar (forming curved surfaces) in the elderly group. Second, the distributions could be essentially planar but with significant noise leading to deviations from a perfect plane (compare a thin flat pancake with a thick one). We assumed that the second scenario was true and applied the same analysis to the data of both groups. We have to admit upfront that this assumption may be wrong but at present we do not have sufficient amounts of data to check the first scenario with adequate power.

When goodness of fit of the computed cost function was tested using direct optimization, the values of the D-angle were very small for the young group (on average <1.5°) while they were significantly higher for the elderly group (about 5°). There is no criterion on what values of the D-angle are "good enough". In earlier studies, some of the young subjects showed data sets resulting in the values of the angle of about 5° (Park et al. 2010). So, this finding by itself is also unable to clearly distinguish between the two scenarios: "Thick pancake versus curved pancake".

The PCA showed several significant differences between the two groups. The two PCs may be interpreted as related to force production (PC1; all loading factors have the same sign) and to moment production (PC2; the loading factors for the *I* and *M* fingers have a sign opposite to that of the loading factors for the *R* and *L* fingers). We would like to focus on a significant difference in the loading coefficients in PC2. In the young group, similarly to earlier studies (Park et al. 2010, 2011), we observed higher absolute magnitudes of those coefficients for the fingers with higher mechanical advantage (*I* and *L*) as compared to the fingers with low mechanical advantage (*M* and *R*). So, we may conclude that performance of the young subjects

was characterized by using the principle of mechanical advantage, which states that elements with higher mechanical advantage are involved to a larger degree in moment production tasks. This principle has been confirmed in studies of both multimuscle joint torque production and multidigit moment of force production (Buchanan et al. 1989; Prilutsky 2000; Zatsiorsky et al. 2003; Zhang et al. 2009).

In contrast, in the elderly, there was no significant difference in the absolute magnitudes of loading coefficients between the "lateral" (IL) fingers and "central" (MR) fingers. In fact, on average, the loading coefficients were slightly larger in absolute magnitude for the MR fingers. This finding allows us to offer a hypothesis that healthy aging is associated with a change in the strategy of sharing moment of force across parallel effectors.

This hypothesis has been confirmed by the analysis of the percentage of the moment produced by the lateral finger (I or L) within finger pairs (IM and RL). Indeed, the young participants used the lateral fingers to produce close to 70% of the total moment produced by a pair of fingers acting in the same direction, while the elderly participants shared the moment of force nearly equally between the fingers with different moment arms (note that the moment arms differed three-fold, 1.5 cm vs. 4.5 cm). Taken together, these analyses show that aging is associated with a switch from using mechanical advantage in moment of force sharing to sharing moment of force nearly equally between contributing fingers irrespective of their mechanical advantages.

There were certain common features in the pattern of coefficients in the J function across the two groups. All subjects showed positive coefficients at the second-order terms (k) and similar patterns of the coefficients at the first-order terms (w), $w < 0$ for the I and L fingers, while $w > 0$ for the M and R fingers. Earlier, an interpretation has been offered for the k and w coefficients (Park et al. 2011). At low forces, the instruction to produce a rather broad range of moments of force favors the use of fingers with large lever arms (I and L). Since first-order terms will have larger effects at the low-force magnitudes, this is reflected in negative values of w for the I and L fingers (their involvement is encouraged). At high forces, for the same range of the moment of force, one has to use fingers with smaller lever arms (M and R). Since at high forces, the contribution of second-order terms increases, k-values are smaller for the MR pair as compared to the IL pair. This contrast was particularly strong for the elderly group (Fig. 3a) suggesting that elderly subjects were more consistent in following the described principle. This conclusion is corroborated by the findings of overall larger involvement of the M and R fingers in moment of force production in the elderly group. We will get back to this seemingly unexpected finding in the next section.

Age effects on multidigit synergies

Within this study, we define synergies as covaried adjustments of elemental variables (finger forces) that stabilize a certain desired value of important performance variables (total force, total moment, or a combination of both) to which all elemental variables contribute (see Latash et al. 2007; Latash 2010a, b). Two characteristics of synergies are commonly quantified, sharing pattern and covariation index. The former is evident in averaged across trials data; it reflects how the subjects share performance variables among elemental variables. The latter is quantified using deviations of elemental variables from average values in individual trials.

Our task required simultaneous production of accurate $\{F_{TOT}; M_{TOT}\}$ combinations. One atypical feature of sharing in the elderly group has been mentioned in the previous section: Unlike the young group, the elderly persons did not show use of the mechanical advantage in moment production. Another unexpected finding related to the sharing pattern in the smaller co-contraction index (CCI) in the elderly group. The term "co-contraction" is more commonly used with respect to simultaneous activation of muscles acting against each other at a joint, so-called agonist–antagonist muscle pairs (Wolf et al. 1994; Slijper and Latash 2000; Hansen et al. 2002; Kellis et al. 2003). In our study, we used this term for digits that acted against each other with respect to M_{TOT} production (see also Zatsiorsky et al. 2002; Shim et al. 2004; Zhang et al. 2006). Lower values of CCI imply seemingly more economic performance. To interpret the finding of lower CCI in the elderly group, consider two factors that could potentially contribute to CCI magnitude.

First, for some tasks, involvement of digits that produced moment of force against the required direction (M_{ANT}) was mechanically necessary. Indeed, if the task value of M_{TOT} was low while F_{TOT} was high, using only agonist fingers could be impossible, and the subjects had to show substantial M_{ANT}. The role of this factor has been supported by the effects of *Force* and *Moment* on CCI (Fig. 4). Since the set of tasks in all the subjects were the same (in %MVC), this factor likely played the same role in the two groups (supported by the lack of interactions of the mentioned factors with the *Age* factor).

Second, when a person tries to produce force with a subset of fingers, other fingers also produce force. This phenomenon has been addressed as lack of individuation or enslaving (Kilbreath and Gandevia 1994; Li et al. 1998; Schieber and Santello 2004). In an earlier paper, M_{ANT} production in prehensile tasks was attributed to both enslaving and mechanical necessity (Zatsiorsky et al. 2002). A number of earlier studies of pressing tasks documented smaller enslaving in the elderly (Shinohara et al.

2003a, b; Kapur et al. 2010). In a recent study, these results in combination with smaller synergy indices, have been used to offer a "back-to-elements" hypothesis (Kapur et al. 2010). This hypothesis assumes that the loss of neurons, including cortical neurons, in elderly persons (Eisen et al. 1996; Christou 2009) results in deterioration of synergic mechanisms and leads to necessity to construct movements based on elements. The idea of a distributed cortical control of the hand (Schieber 2001; Schieber and Santello 2004) with individual cortical neurons being able to induce activation changes in many different muscles (divergence) and numerous, broadly distributed neurons projecting on the same muscle or effector (convergence) assumes the availability of a hugely redundant set of neurons. When neuronal redundancy decreases with age, a shift toward more focused, somatotopic control scheme may happen resulting in better individuated finger control reflected in lower enslaving indices. The unexpectedly lower CCI in the elderly group of our study may be a consequence of the same processes and the lower enslaving.

There is another interpretation of the lower CCI in the elderly group; it follows the idea of chain effects, which are sequences of mechanically necessitated cause-consequence couples in a multielement system (see Zatsiorsky et al. 2002, 2003; Shim et al. 2005a). The following chain effects can be traced. (a) The elderly persons produced smaller shares of the moment of force by lateral fingers, i.e., smaller $\%M_{\mathrm{AGO\_Lateral}}$ and $\%M_{\mathrm{ANT\_Lateral}}$, as compared to those produced by the young subjects (see Fig. 5). (b) This means that they produced larger forces by the central fingers (M and R fingers) in order to reach required $\mathrm{F_{TOT}}$ levels. (c) Such a sharing pattern, which does not use the principle of mechanical advantage, requires producing higher total force by a finger pair (IM or RL) that generates moment of force in the required direction (M_{AGO}). (d) As a result, to produce a required total force for a given moment of force, the moment antagonists have to produce a smaller force. (e) This leads to smaller co-contraction indices.

The application of the method based on the UCM hypothesis (Scholz and Schöner 1999) to analyze multidigit synergies confirmed earlier reports on lower synergy indices in older persons (Shinohara et al. 2003a, b, 2004; Shim et al. 2004). The analysis of the two variance components, V_{UCM} and V_{ORT}, has shown that the drop in the synergy index with age is primarily associated with a disproportionate increase in $\mathrm{V_{ORT}}$, while both $\mathrm{V_{ORT}}$ and $\mathrm{V_{UCM}}$ increase. The difference between the two groups was particularly strong at higher forces confirming earlier observations (Shinohara et al. 2003a, b; Shim et al. 2004). In this study, we used finger forces as elemental variables in the analyses of synergies while the cited earlier studies of age effects on synergies were performed in the space of hypothetical commands to fingers, finger modes (Latash et al. 2001; Danion et al. 2003). Finger modes are defined as commands to a finger that result in force production by all the fingers of the hand intended and unintended. Unintended finger force production (enslaving, Li et al. 1998; Zatsiorsky et al. 2000) has been shown to be lower in elderly persons (Shinohara et al. 2003a, b; Kapur et al. 2010). Since enslaving, by definition, contributes to positive covariation of finger forces, persons with higher enslaving are expected to show lower indices of force-stabilizing synergies, other factors being equal. Since higher enslaving was expected in the young group, our computation underestimated the age-related drop in the synergy indices. We did not switch in our synergy analysis to finger modes to be consistent in the variables used in the synergy and ANIO parts of the study.

The synergy index ΔV was positive in all the subjects and for all the analyses. The finding $\Delta V > 0$ is a sign of covariation among elemental variables (finger forces) that keeps the performance variable, for which analysis has been run, relatively unchanged. In other words, this finding means a multielement synergy stabilizing that performance variable. This result shows that there was only a quantitative difference in the performance of the two groups: Both groups were able to stabilize both F_{TOT} and M_{TOT} simultaneously as documented in earlier studies for young persons (Zhang et al. 2009; Park et al. 2010).

Links between optimality and variability

Since we cannot draw 4D figures on a 2D piece of paper, we will illustrate the main ideas linking the ANIO and UCM approaches using a different task with only two elements and one constraint: Total force (F_{TOT}) production by two fingers (see the "Introduction" and Fig. 8; see also Latash 2008). In this example, the UCM represents a slanted line with a negative slope (thin, solid lines). For different values of F_{TOT}, the UCMs are parallel to each other. This is also true for the UCMs for different $\{F_{\mathrm{TOT}}; M_{\mathrm{TOT}}\}$ combinations in the task used in the current study. The line orthogonal to the UCM (thin, dashed line) is the direction of "bad variability" (V_{ORT}). Six distributions of data points are shown with ellipses that differ in their sharing pattern (the locations of the centers of the distributions) and the amounts of V_{UCM} and V_{ORT}. Note that $V_{\mathrm{UCM}} > V_{\mathrm{ORT}}$ for all distributions (meaning that $\Delta V > 0$), while both variance components are higher for the distributions marked E (elderly) as compared to the ones marked Y (young). Note also that the E distributions are more circular as compared to the Y ones. Overall, this figure reflects the main differences found between the young and elderly groups in our study: Different sharing patterns, synergies stabilizing performance variables in both groups,

higher variance in the elderly group, and lower synergy index in the elderly group.

We assume that average locations of the data points (the sharing pattern) reflect an optimization process (note that moment of force production is not considered in this example!). If the same optimization principle defines sharing patterns across a range of F_{TOT}, a line connecting the centers of all those distributions is the sub-space of optimal solutions (thick dashed lines in Fig. 8). Note that this line does not have to be orthogonal to the UCM. If F_{TOT} is shared evenly between the two fingers, the angle between the two lines is exactly 90°. Deviations of this angle from 90° reflect deviations of the sharing pattern from 50:50. If all human fingers were identical with identical lever arms, one could expect the angle between the UCM and the plane of optimal solutions measured in our study to be 90° for optimal performance. The fact that this angle differs from 90° even in young healthy persons (see also Terekhov et al. 2010; Park et al. 2010) likely reflects the fact that the four fingers differ in their force producing capability as well as in the lever arms. We assume that performance of young subjects was optimal (assuming that there is such a thing as optimal performance). Hence, further deviations of the angle from 90° reflect a change in the sharing pattern that deviates the performance from optimal more.

The two subject groups in our study showed overlapping ranges in virtually all outcome variables despite the significant differences between the groups. When all the data across all the subjects were analyzed together, significant correlations were found between the index of synergy (ΔV) based on session-2 and indices computed using the data from session-1. We have to admit that for this analysis we combined the data from the two groups; this might have affected the results, although the data point distributions in the two groups did not form two separate clouds but showed a substantial overlap. The results suggest that smaller synergy indices (computed across repetitions of the same task!) correspond to less planar data (across multiple tasks!) and larger deviations of the plane of optimal solutions from the plane of experimental data. The two analyses, of optimal performance over multiple tasks and of force covariation over trials at one task, are likely to reflect a single set of processes associated with healthy aging. This process leads to potentially suboptimal sharing patterns and weaker synergies.

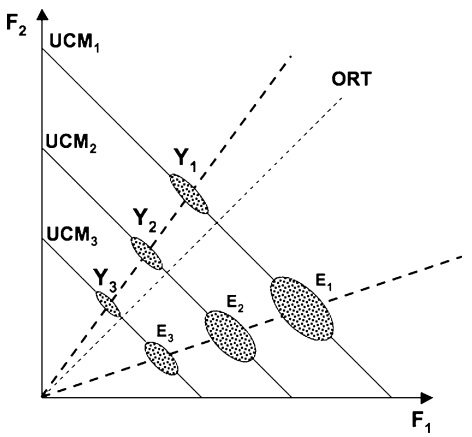

Fig. 8 An illustration of data distributions in a task of accurate total force production with two fingers pressing in parallel. In the space of finger forces {F_1; F_2}, the solid thin lines show the uncontrolled manifolds (UCMs) for this task corresponding to different magnitudes of the total force. The orthogonal to the UCMs direction is shown with the thin, *dashed line*. Six data distributions are shown that differ in the sharing patterns and amounts of variance; they illustrate the main differences in our study between the young (*Y*) and elderly (*E*) groups. The *thick, dashed lines* show the direction of preferred solutions

We would like to mention a few limitations of the study. First, the force/moment production tasks used in this study were not very similar to everyday tasks. We used them primarily because they allowed to impose two constraints on the four-finger system and explore its behavior within a wide range of constraint values. On the other hand, the tasks of total normal force and total moment of force production are rather common, for example during taking a sip from the glass. In such, more natural, tasks, however, total moment of force is a crucial variable, not the moment produced by the normal forces. So, we view the current task as a reasonable approximation of everyday prehensile tasks, a first step that will ultimately lead to using more ecologically valid tasks. In general, the combination of the ANIO method and the UCM-based analysis of synergies can be used for different sets of elemental variables and constraints.

Second, it is possible that the subject groups differed in the percentage of "true" maximal force they generated during the MVC tests; this could have an effect on several of the outcome variables. In studies like this one, researchers always rely on full cooperation by the subjects, in particular on their performance in MVC tasks at 100% of effort. The MVC values, we observed (71.6 ± 11.3 N in the young group and 51.3 ± 5.25 N in the elderly group) were not much different from those in earlier studies that used a similar setup (Shinohara et al. 2003a; Kapur et al. 2010). So, we trust that the underproduction in the MVC tests was not a major factor.

Third, we provided similar amounts of practice for the young and elderly groups. Given evidence that older adults may learn new motor skills slower (reviewed in Light 1990), it is possible that they were disadvantaged by this element of the experimental design. In this study, we did not explore effects of different amounts of practice on the outcome indices, and this seems a natural future development of this line of research.

Acknowledgments We are grateful to Dr. Alexander Terekhov for his help. The study was supported in part by NIH grants AG-018751, NS-035032, and AR-048563.

Appendix 1

Analytical Inverse Optimization (ANIO) approach

The optimization problem in the current study was defined as

$$\text{Min} \quad J = \sum_{i=1}^{4} g_i(F_i) \tag{8}$$

$$\text{Subject to} \quad \begin{array}{c} F_i + F_m + F_r + F_l = a \cdot \text{MVC}_{\text{IMRL}} \\ d_i \cdot F_i + d_m \cdot F_m + d_r \cdot F_r + d_l \cdot F_l = b \cdot 0.07 \cdot d_i \cdot \text{MVC}_I \end{array}$$

The two linear constraints are expressed as

$$CF^T = B \tag{9}$$

$$F = [F_i \quad F_m \quad F_r \quad F_l]$$

$$C = \begin{bmatrix} 1 & 1 & 1 & 1 \\ d_i & d_m & d_r & d_l \end{bmatrix}$$

$$B = \begin{bmatrix} F_{\text{TOT}} \\ M_{\text{TOT}} \end{bmatrix}$$

The task involved two constraints (F_{TOT} and M_{TOT} values) and four elemental variables (finger forces). Thus, the solutions of this undetermined system were expected to be confined to a two-dimensional surface in the four-dimensional force space. Planarity of this surface was checked using the PCA. The following computational procedure explains how the optimization cost function is obtained.

First, we identify whether the optimization problem is splittable or not by observing the (4 × 4) matrix:

$$\breve{C} = I - C^T(CC^T)^{-1}C \tag{10}$$

Second, we check whether the experimental data actually lie on a hyperplane (and not for instance on a curved hypersurface) and then define the observed hyperplane mathematically as

$$A \cdot F^T = b \tag{11}$$

where A is a 2 × 4 matrix composed of the transposed vectors of the two lesser principal components obtained from the PCA from the finger force data in session-1. A large percentage of the total variance explained by the two first principal components was considered an indicator that the data lie on a hyperplane. However, the data points were not perfectly confined to a plane due to the variability of performance and instrumental noise. Also, the plane computed from Eq. 11 is affected by experimental errors.

Third, we compare the experimentally determined hyperplane to the theoretical plane derived from the Uniqueness Theorem. The experimental data must be fitted by the following equation:

$$\breve{C}f'(F) = 0, \tag{12}$$

where $f'(F) = \left(f_1'(F_i), f_2'(F_m), f_3'(F_r), f_4'(F_l)\right)^T f_i$ are arbitrary continuously differentiable functions. At the second step, the data are discovered to lie on the plane and hence the functions $fi'(\cdot)$ are linear:

$$f_i'(F_i) = k_i F_i + w_i \tag{13}$$

where $i = \{index, middle, ring, and\ little\}$. Therefore,

$$f_i(F_i) = \frac{k_i}{2}(F_i)^2 + w_i F_i \tag{14}$$

The values of the coefficients of the second-order terms k_i can be determined by minimizing the dihedral angle between the two planes: the plane of optimal solutions $\breve{C}f'(F) = 0$ and the plane of experimental observations ($A \cdot F^T = 0$). The values of the coefficients of the first-order terms w_i were found to correspond to a minimal vector length ($w = (w_{\text{index}}, w_{\text{middle}}, w_{\text{ring}}, w_{\text{little}})^T$) bringing the theoretical and the experimental plane as close to each other as possible. Vector w satisfy the following equation:

$$\breve{C}f'(F) = \breve{C}(KF_i + w) \tag{15}$$

where $K = (k_{\text{index}}, k_{\text{middle}}, k_{\text{ring}}, k_{\text{little}})^T$ and $w = (w_{\text{index}}, w_{\text{middle}}, w_{\text{ring}}, w_{\text{little}})^T$.

Then, the functions g_i in Eq. 10 are the following:

$$g_i(x_i) = rf_i(F_i) + q_i F_i + \text{const}_i \tag{16}$$

where r is a non-zero number, const_i can be any real number, and q_i is any real number satisfying the equation $\breve{C}q = 0$ (Terekhov et al. 2010). Multiplication of the cost function by a constant value or adding a constant value to it does not change the cost function essentially. Hence, we can arbitrary assume that $r = 1$ and $\text{const}_i = 0$. According to the Uniqueness Theorem, identification of the cost function can be performed only up to unknown linear terms which are parameterized by the values q_i. We assume that $q_i = 0$ in order to simplify $g_i(x_i)$. It must be kept in mind, however, that the true cost function used by the CNS might have these terms.

Uniqueness theorem (for the mathematical proof see Terekhov et al. 2010)

The core of the ANIO approach is the theorem of uniqueness that specifies conditions for unique (with some

restrictions) estimation of the objective functions. The main idea of the theorem of uniqueness is to find necessary conditions for the uniqueness of solutions in an inverse optimization problem. An optimization problem (i.e., direct optimization problem) with an additive objective function and linear constraints are defined as:

$$\begin{aligned} &\text{Let J} : R^n \rightarrow R^1 \\ &\text{Min} : J(x) = g_1(x_1) + g_2(x_2) + \cdots + g_n(x_n) \\ &\text{Subject to} : CX^T = B \end{aligned} \tag{17}$$

where $X = (x_1, x_2, \ldots, x_n) \backslash, \in R^n$, g_i is an unknown scalar differentiable function with $g'(\bullet) > 0$. g_i came from the Lagrange minimum principle, which has a unique solution. On the contrary, the functions of g_i can be computed from the set of solutions X^* (e.g., experimental data). This inverse procedure is called the inverse optimization problem. C is a $k \times n$ matrix and B is a k-dimension vector, $k < n$.

First, assume that the optimization problem (Eq. 17) with $k \geq 2$ is non-splittable. If the inverse optimization is splittable, the preliminary step is to split it until a non-splittable subproblem is acquired. If the functions $g_i(x_i)$ in problem (Eq. 17) are twice continuously differentiable (i.e., twice continuously differentiable functions f_i) and f_i' is not identically constant, complying $\breve{C}f'(X) = 0$ for all $X \in X^*$,

$$f'(X) = \left(f_1'(x_1), \cdots, f_n'(x_n)\right)^T \tag{18}$$

$$\text{and } \breve{C} = I - C^T(CC^T)^{-1}C \tag{19}$$

$$\text{then } g_i(x_i) = rf_i(x_i) + q_i x_i + \text{const}_i \tag{20}$$

for every $x_i \in X_i^*$, where $X_i^* = \{s |$ there is $X \in X^*$: $x_i \in s\}$ and X^* is the set of the solutions for all $B \in R^k$. The constants q_i satisfy the equation $\breve{C}q = 0$ where $q = (q_1, \cdots, q_n)^T$. Primes designate derivatives.

If the experimental data correspond to solutions of an inverse optimization problem with additive objective function (g_i) and linear constraints, equation $\breve{C}f'(X) = 0 (X \in X^*)$ must be satisfied (i.e., the Lagrange principle). The Uniqueness Theorem provides sufficient condition (i.e., $\breve{C}f'(X) = 0$) for solving the inverse optimization problem in a unique way up to linear terms.

Appendix 2

Uncontrolled manifold (UCM) analysis (see Latash et al. 2002; Scholz et al. 2002 for details)

For F_{TOT}, changes in the elemental variables (finger forces) sum up to produce a change in F_{TOT}:

$$dF_{\text{TOT}} = [\,1 \quad 1 \quad 1 \quad 1\,] \cdot [\,dF_i \quad dF_m \quad dF_r \quad dF_l\,]^T \tag{21}$$

The UCM was defined as an orthogonal set of the vectors e_i in the space of the elemental forces that did not change the net normal force, i.e.,:

$$0 = [\,1 \quad 1 \quad 1 \quad 1\,]e_i \tag{22}$$

These directions were found by taking the null-space of the Jacobian of this transformation ([1 1 1 1] e_i). The mean-free forces were then projected onto these directions and summed to produce:

$$f_{||} = \sum_i^{n-p} \left(e_i^T \cdot df\right)e_i, \tag{23}$$

where $n = 4$ is the number of degrees-of-freedom of the elemental variables, and $p = 1$ is the number of degrees-of-freedom of the performance variable (F_{TOT}). The component of the de-meaned forces orthogonal to the null-space is given by:

$$f_{\perp} = df - f_{||} \tag{24}$$

The amount of variance per degree of freedom parallel to the UCM is:

$$V_{\text{UCM}} = \frac{\sum |f_{||}|^2}{(n-p)N_{\text{trials}}} \tag{25}$$

The amount of variance per degree of freedom orthogonal to the UCM is :

$$V_{\text{ORT}} = \frac{\sum |f_{\perp}|^2}{pN_{\text{trials}}} \tag{26}$$

The normalized difference between these variances is quantified by a variable ΔV:

$$\Delta V = \frac{V_{\text{UCM}} - V_{\text{ORT}}}{V_{\text{TOT}}} \tag{27}$$

where V_{TOT} is the total variance, also quantified per degree-of-freedom. If ΔV is positive, $V_{\text{UCM}} > V_{\text{ORT}}$, caused by negative covariation of the finger forces, which we interpret as evidence for a force-stabilizing synergy. In contrast, $\Delta V = 0$ indicates independent variation of the finger forces, while $\Delta V < 0$ indicates positive covariation of the individual finger forces, which contributes to variance of F_{TOT}.

A similar procedure was used to compute the two variance components related to stabilization of M_{TOT}. The only difference was in using a different Jacobian corresponding to the lever arms of individual finger forces, [d_i d_m d_r d_l].

We also analyzed the data with respect to stabilization of both F_{TOT} and M_{TOT} simultaneously. In that case, the Jacobian was [1 1 1 1 d_i d_m d_r d_l]. The dimensionality of

V_{UCM} for the analysis with respect to F_{TOT} and M_{TOT} separately is three (one constraint), while the dimensionality of V_{UCM} with respect to F_{TOT} and M_{TOT} simultaneously is two (two constraints).

References

Bernstein NA (1967) The co-ordination and regulation of movements. Pergamon Press, Oxford

Booth FW, Weeden SH, Tseng BS (1994) Effect of aging on human skeletal muscle and motor function. Med Sci Sports Exerc 26:556–560

Brooks SV, Faulkner JA (1994) Skeletal muscle weakness in old age: underlying mechanisms. Med Sci Sports Exerc 26:432–439

Buchanan TS, Rovai GP, Rymer WZ (1989) Strategies for muscle activation during isometric torque generation at the human elbow. J Neurophysiol 62:1201–1212

Burnett RA, Laidlaw DH, Enoka RM (2000) Coactivation of the antagonist muscle does not covary with steadiness in old adults. J Appl Physiol 89:61–71

Christou EA (2009) Aging and neuromuscular adaptations with practice. In: Shinohara M (ed) Advances in neuromuscular physiology of motor skills and muscle fatigue. Research Signpost, Kerala, pp 65–79

Cole KJ (1991) Grasp force control in older adults. J Mot Behav 23:251–258

Cole KJ, Rotella DL, Harper JG (1999) Mechanisms for age-related changes of fingertip forces during precision gripping and lifting in adults. J Neurosci 19:3238–3247

Contreras-Vidal JL, Teulings HL, Stelmach GE (1998) Elderly subjects are impaired in spatial coordination in fine motor control. Acta Psychol (Amst) 100:25–35

Cooke JD, Brown SH, Cunningham DA (1989) Kinematics of arm movements in elderly humans. Neurobiol Aging 10:159–165

Danion F, Schöner G, Latash ML, Li S, Scholz JP, Zatsiorsky VM (2003) A force mode hypothesis for finger interaction during multi-finger force production tasks. Biol Cybern 88:91–98

Dinse HR (2006) Cortical reorganization in the aging brain. Prog Brain Res 157:57–80

Doherty TJ, Brown WF (1997) Age-related changes in the twitch contractile properties of human thenar motor units. J Appl Physiol 82:93–101

Eisen A, Entezari-Taher M, Stewart H (1996) Cortical projections to spinal motoneurons: changes with aging and amyotrophic lateral sclerosis. Neurology 46:1396–1404

Enoka RM, Christou EA, Hunter SK, Kornatz KW, Semmler JG, Taylor AM, Tracy BL (2003) Mechanisms that contribute to differences in motor performance between young and old adults. J Electromyogr Kinesiol 13:1–12

Erim Z, Beg FM, Burke DT, De Luca CJ (1999) Effects of aging on motor-unit control properties. J Neurophysiol 82:2081–2091

Francis KL, Spirduso WW (2000) Age differences in the expression of manual asymmetry. Exp Aging Res 26:169–180

Gelfand IM, Latash ML (1998) On the problem of adequate language in movement science. Mot Control 2:306–313

Gorniak SL, Zatsiorsky VM, Latash ML (2007) Hierarchies of synergies: an example of two-hand, multifinger tasks. Exp Brain Res 179:167–180

Gorniak SL, Zatsiorsky VM, Latash ML (2009) Hierarchical control of prehension. II. Multi-digit synergies. Exp Brain Res 194:1–15

Grabiner MD, Enoka RM (1995) Changes in movement capabilities with aging. Exerc Sport Sci Rev 23:65–104

Hansen S, Hansen NL, Christensen LO, Petersen NT, Nielsen JB (2002) Coupling of antagonistic ankle muscles during co-contraction in humans. Exp Brain Res 146:282–292

Hughes S, Gibbs J, Dunlop D, Edelman P, Singer R, Chang RW (1997) Predictors of decline in manual performance in older adults. J Am Geriatr Soc 45:905–910

Kaiser HF (1960) The application of electronic computers to factor analysis. Psychol Measures 20:141–151

Kang N, Shinohara M, Zatsiorsky VM, Latash ML (2004) Learning multi-finger synergies: an uncontrolled manifold analysis. Exp Brain Res 157:336–350

Kapur S, Zatsiorsky VM, Latash ML (2010) Age-related changes in the control of finger force vectors. J Appl Physiol 109:1827–1841

Kellis E, Arabatzi F, Papadopoulos C (2003) Muscle co-activation around the knee in drop jumping using the co-contraction index. J Electromyogr Kinesiol 13:229–238

Kilbreath SL, Gandevia SC (1994) Limited independent flexion of the thumb and fingers in human subjects. J Physiol 479:487–497

Latash ML (2008) Synergy. Oxford University Press, New York

Latash ML (2010a) Motor synergies and the equilibrium-point hypothesis. Mot Control 14:294–322

Latash ML (2010b) Motor control: in search of physics of the living systems. J Hum Kinet 24:7–18

Latash ML, Scholz JF, Danion F, Schöner G (2001) Structure of motor variability in marginally redundant multi-finger force production tasks. Exp Brain Res 141:153–165

Latash ML, Scholz JP, Schöner G (2002) Motor control strategies revealed in the structure of motor variability. Exerc Sport Sci Rev 30:26–31

Latash ML, Scholz JP, Schöner G (2007) Toward a new theory of motor synergies. Mot Control 11:276–308

Levinson DJ (1978) Seasons of a man's life. Knopf, New York

Li ZM, Latash ML, Zatsiorsky VM (1998) Force sharing among fingers as a model of the redundancy problem. Exp Brain Res 119:276–286

Light KE (1990) Information processing for motor performance in aging adults. Phys Ther 70:820–826

Nelson W (1983) Physical principles for economies of skilled movements. Biol Cybern 46:135–147

Olafsdottir H, Yoshida N, Zatsiorsky VM, Latash ML (2005) Anticipatory covariation of finger forces during self-paced and reaction time force production. Neurosci Lett 381:92–96

Olafsdottir H, Zhang W, Zatsiorsky VM, Latash ML (2007) Age-related changes in multi-finger synergies in accurate moment of force production tasks. J Appl Physiol 102:1490–1501

Oldfield RC (1971) The assessment and analysis of handedness: the Edinburgh inventory. Neuropsychologia 9:97–113

Park J, Zatsiorsky VM, Latash ML (2010) Optimality versus variability: an example of multi-finger redundant tasks. Exp Brain Res 207:119–132

Park J, Zatsirosky VM, Latash ML (2011) Finger coordination under artificial changes in finger strength feedback: a study using analytical inverse optimization. J Mot Behav 43:229–235

Prilutsky BI (2000) Coordination of two- and one-joint muscles: Functional consequences and implications for motor control. Mot Control 4:1–44

Rantanen T, Guralnik JM, Foley D, Masaki K, Leveille S, Curb JD, White L (1999) Midlife hand grip strength as a predictor of old age disability. JAMA 281:558–560

Rogers MA, Evans WJ (1993) Changes in skeletal muscle with aging: effects of exercise training. Exerc Sport Sci Rev 21:65–102

Schieber MH (2001) Constraints on somatotopic organization in the primary motor cortex. J Neurophysiol 86:2125–2143

Schieber MH, Santello M (2004) Hand function: peripheral and central constraints on performance. J Appl Physiol 96: 2293–2300

Scholz JP, Schöner G (1999) The uncontrolled manifold concept: identifying control variables for a functional task. Exp Brain Res 126:289–306

Scholz JP, Danion F, Latash ML, Schöner G (2002) Understanding finger coordination through analysis of the structure of force variability. Biol Cybern 86:29–39

Seidler-Dobrin RD, He J, Stelmach GE (1998) Coactivation to reduce variability in the elderly. Mot Control 2:314–330

Shim JK, Lay B, Zatsiorsky VM, Latash ML (2004) Age-related changes in finger coordination in static prehension tasks. J Appl Physiol 97:213–224

Shim JK, Latash ML, Zatsiorsky VM (2005a) Prehension synergies in three dimensions. J Neurophysiol 93:766–776

Shim JK, Olafsdottir H, Zatsiorsky VM, Latash ML (2005b) The emergence and disappearance of multi-digit synergies during force production tasks. Exp Brain Res 164:260–270

Shinohara M, Latash ML, Zatsiorsky VM (2003a) Age effects on force produced by intrinsic and extrinsic hand muscles and finger interaction during MVC tasks. J Appl Physiol 95:1361–1369

Shinohara M, Li S, Kang N, Zatsiorsky VM, Latash ML (2003b) Effects of age and gender on finger coordination in MVC and sub-maximal force-matching tasks. J Appl Physiol 94:259–270

Shinohara M, Scholz JP, Zatsiorsky VM, Latash ML (2004) Finger interaction during accurate multi-finger force production tasks in young and elderly persons. Exp Brain Res 156:282–292

Slijper H, Latash ML (2000) The effects of instability and additional hand support on anticipatory postural adjustments in leg, trunk, and arm muscles during standing. Exp Brain Res 135:81–93

Terekhov AV, Pesin YB, Niu X, Latash ML, Zatsiorsky VM (2010) An analytical approach to the problem of inverse optimization with additive objective functions: an application to human prehension. J Math Biol 61:423–453

Verrillo RT (1979) Change in vibrotactile thresholds as a function of age. Sens Processes 3:49–59

Walker N, Philbin DA, Fisk AD (1997) Age-related differences in movement control: adjusting submovement structure to optimize performance. J Gerontol B Psychol Sci Soc Sci 52:P40–52

Welford AT (1984) Between bodily changes and performance: some possible reasons for slowing with age. Exp Aging Res 10:73–88

Wolf SL, Catlin PA, Blanton S, Edelman J, Lehrer N, Schroeder D (1994) Overcoming limitations in elbow movement in the presence of antagonist hyperactivity. Phys Ther 74:826–835

Zatsiorsky VM, Li ZM, Latash ML (2000) Enslaving effects in multi-finger force production. Exp Brain Res 131:187–195

Zatsiorsky VM, Gregory RW, Latash ML (2002) Force and torque production in static multifinger prehension: biomechanics and control. II. Control. Biol Cybern 87:40–49

Zatsiorsky VM, Gao F, Latash ML (2003) Prehension synergies: effects of object geometry and prescribed torques. Exp Brain Res 148:77–87

Zhang W, Zatsiorsky VM, Latash ML (2006) Accurate production of time-varying patterns of the moment of force in multi-finger tasks. Exp Brain Res 175:68–82

Zhang W, Olafsdottir HB, Zatsiorsky VM, Latash ML (2009) Mechanical analysis and hierarchies of multidigit synergies during accurate object rotation. Mot Control 13:251–279